International Forum on Aeroelasticity and Structural Dynamics
IFASD 2026
16-19 June 2026, Göttingen, Germany

AEROELASTIC OPTIMIZATION FOR DYNAMIC MODEL ADJUSTMENT BASED ON GROUND- / FLIGHT TEST DATA AND INCREASED STABILITY MARGIN

Wolf R. Krüger[1*], Andreas Senft[2], Björn-Ole Schröder[1], Frank Schröder[2]

[1]DLR – Institute of Aeroelasticity, Bunsenstr. 10, 37073 Göttingen, Germany
[*]Wolf.Krueger@DLR.de

[2]Airbus Operations GmbH, Airbus-Allee 1, 28199 Bremen, Germany

Keywords: structural dynamics, finite element model update, flutter optimization, GVT, FVT

Abstract:

In the context of aeroelastic stability assessment, the development of a reliable Finite Element Model (FEM) is paramount for ensuring aircraft safety and performance. This paper presents a comprehensive approach to dynamic model adjustment and aeroelastic optimization, integrating ground vibration test and flight vibration test data within a unified optimization framework. The proposed methodology, implemented via the NASTRAN optimization module, enables simultaneous calibration of numerical models to both ground and flight test data, overcoming previous limitations that restricted adjustments to GVT. The framework now supports the inclusion of effects from FVT (aerodynamics), and allows the adaptation of distributed design fields of wing, fuselage and empennage for more accurate representation of the aeroelastic behaviour.

The Dynamic Model Adjustment Optimization (DynAOPT) process is demonstrated on a civil transport test aircraft, where transfer functions, particularly rudder-to-cockpit responses, were used as validation targets. Optimization was performed across multiple frequency bands, including frequencies up to 10 Hz, approximately. The results show significant improvement in correlation between test data and simulation, especially in amplitude and frequency matching, with the optimized model successfully eliminating unphysical peaks observed in the baseline model. Notably, the use of move limits on design variables was shown to influence both convergence behaviour and the distribution of stiffness and damping adjustments, highlighting the importance of constraint definition.

Furthermore, the paper addresses the challenge of increasing aeroelastic stability margins through structural optimization, using the same optimization tool environment. A case study on a transport aircraft wing model demonstrates the successful increase of flutter speed by 5% through targeted modifications of wing skin thickness, with minimal mass increase. The optimization was conducted on an isolated wing model to simplify the analysis, with results successfully transferred to the full aircraft model, yielding a 4.62% increase in flutter velocity. This confirms the efficiency and scalability of the approach.

1 INTRODUCTION

In the frame of aeroelastic stability assessment, a reliable Finite Element Model (FEM) is an essential component. Such a model is usually provided by the responsible Stress teams linked with the associated masses of the components given by the Weight department. For the aeroelastic stability assessment, the dynamic model is composed, which is then the basis to derive the modal behaviour in form of frequencies and mode shapes.

An FEM can be modified by changing its elements, for example element stiffness or mass. This can be done having two different objectives in mind. First, property changes are used to adjust the dynamic model to meet test results. Second, changes of element properties can be applied to propose an aircraft design with increased aeroelastic stability margins.

Addressing the first of these objectives, the adjustment of the dynamic model in the verification and validation (V&V) phase of an aircraft, is currently done in two steps. The first step is focussing on the behaviour during Ground Vibration Test (GVT) which allows not only to capture the frequencies and mode shapes of the real aircraft, but also to derive the structural damping associated to each of the identified modes. In this process step, it is possible to concentrate on the structural parameters to achieve an acceptable matching of the test results while having no interference with aerodynamic forces. The second part of the V&V phase is the Flight Vibration Test (FVT) with different fuel / ballast configurations and at various Mach numbers and speeds to identify the evolution of frequency and damping versus speed.

In the past, the adaptation process was mainly focussing on the quality of frequency and mode shape correlation in the lower frequency band using approved stiffness changes as parameters. This is not sufficient in view of future aircraft development programs with much higher mode density in the low frequency domain. Especially for the purpose of control law design, the dynamic model quality has to be improved considerably. The deficiencies of a dynamic model for that purpose can be assessed on the basis of a transfer function approach. The identification of parameters for the model adjustment in this context is key to achieve highest quality in matching test results.

Dynamic model adjustment can be done with the help of optimization. A tool having been used extensively to meet results gained from ground test is the NASTRAN solution SOL200. The reason for having to restrict the adjustment in the past to ground test results was the lack of opportunity to introduce highly accurate aerodynamics into NASTRAN SOL200. This shortcoming has been overcome by using a Least Square Approach altered into the solution sequence being able now to also support flight tests. Therefore, it is now possible to use the large variety of numerical approaches available in SOL200 in combination with several optimization options.

Furthermore, the NASTRAN environment offers features allowing to define several subcases within one optimization run specifying excitations at different driving point locations and imposing constraints at various output stations to consider a set of transfer functions which are relevant for instance for control law design.

Prerequisite for a meaningful adjustment of a dynamic model is that the basis model is representing a feasible design, i.e. being in line with certification requirements. If this is not the case, a step before the adjustment phase could be necessary to improve the aeroelastic behaviour by increasing the flutter speed or increasing the damping of a specific mode. For this purpose, the same elements will be used to propose design recommendations by means of the same tool environment.

As soon as a feasible design is found and approved by the Stress team, the subsequent adjustment step in the V&V phase needs to limit the changes introduced in order to match the test results. This is reflected in the optimization set-up by defining the objective function going to be minimized in such a manner that it incorporates the changes expended for the adjustment. With this objective function definition, it is ensured that the adjustment is not bringing the dynamic model back to be an infeasible solution. With this, the development as well as the verification and validation phase are supported by the same tool environment. Section 2 outlines the process and shows an example for model adaptation.

Certification rules require the airframer to demonstrate that the aircraft is free from flutter at all points of the operational envelope, up to dive speed, plus a margin of 15% over dive speed. This is usually demonstrated by numerical analysis, where the applied numerical model is validated against data from the ground vibration and flight vibration test, as mentioned in Section 2. The risk of encountering a flutter instability late in the design process increases, ultimately results in very costly changes and degraded efficiency. Considering that the development costs of a new aircraft reach billions of dollars, this is a risk to avoid. In addition, there are also derivative aircraft or unforeseen changes in the development that do not allow to include flutter constraints covering all possible configuration variations in advance so a re-design due to existing flight envelope specification might be required. It is thus desirable to have an option to adapt the structure of the aircraft such that the flutter point can be kept outside the certification envelope, and to do that with minimum mass increase, minimum modification of the given aircraft structure, and of course, satisfying all local strength constraints. For typical flutter cases, adaptations of the pylon stiffness of the engine or of the wing skin can be options to modify the global dynamics with minimum structural impact.

For this purpose, the NASTRAN internal optimization routine SOL200 can be applied with a very similar approach as for the GVT / FVT adaptation described above. A structural optimization is used to modify a given structure to take aeroelastic constraints like the flutter point as well as the mentioned constraints (mass, strength limit) into account. This methodology has been demonstrated for a research aircraft configuration and is described in Section 3.

2 DYNAMIC MODEL ADJUSTMENT BASED ON GROUND- AND FLIGHT TEST

2.1 Current Way of Working

For the validation and a potential adaptation of the dynamic model, several data sources are available, Figure 1. The numerical source is a finite element model of medium complexity, i.e. of sufficient detail to represent the frequency range of interest. This model is the so-called Dynamic Master Model (DMM). Experimental data is available from ground vibration tests, which might differ in complexity, depending on the investigation scope - from full scale testing of the overall aircraft for a new aircraft type, to vibration tests focussing on a component, e.g. for a modification of the aircraft to be certified. Finally, data is obtained from flight vibration tests, required for each new aircraft type. While from a GVT information of the structural dynamics are obtained (with the added complexity of boundary conditions which cannot be fully representative for the flying aircraft), the FVT delivers data of the aerodynamic impact on the aeroelastic system, in addition to “real-life” influence from engines running and control systems in the loop.

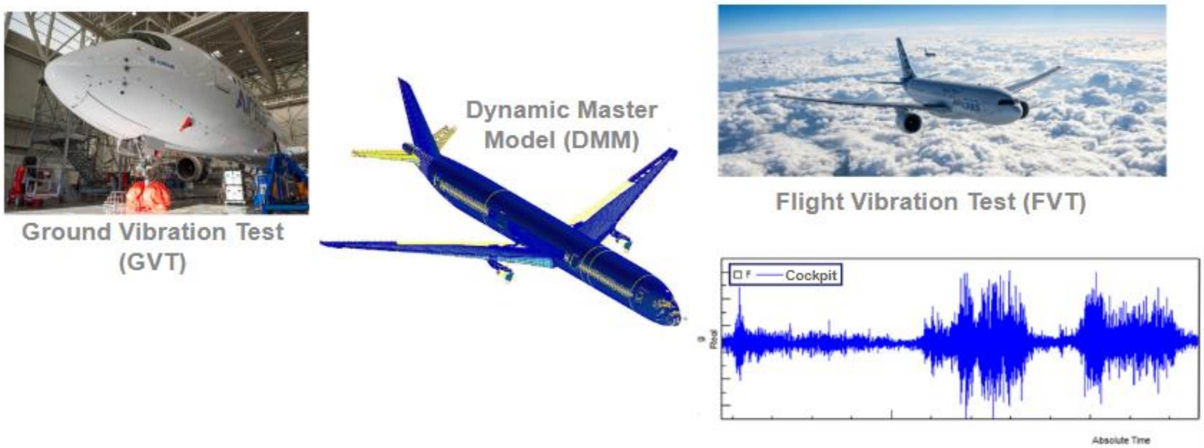

Figure 1. Data sources for model validation

In the current process for dynamic model adjustment, global stiffness modifications concerning the main structures are introduced in the finite element model by means of an additional so-called “stick system” (i.e. beam elements), following the flexural axis of the components and coupled to the structure, see Figure 2. The beam parameters are modified such that global properties of the extended DMM match the data from GVT and FVT as well as possible.

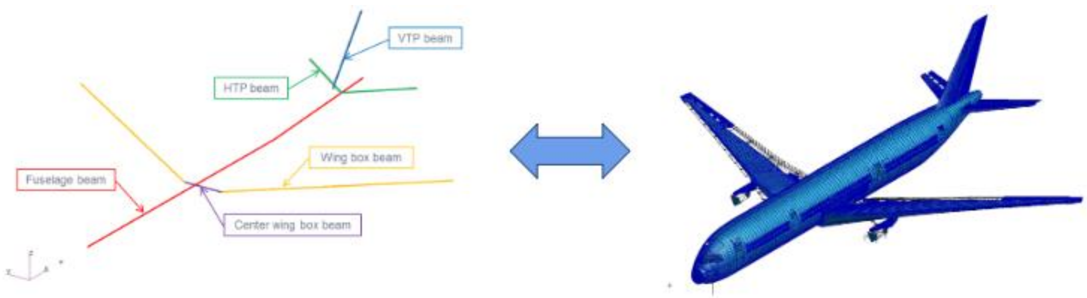

Figure 2. Current process for model update

The following Figure 3 gives an example of the correlation of test results versus simulation model results for data obtained from ground data, from low Mach number flight and from a high Mach number flight. When comparing the numerical model, in the following also called “theoretical model” (TM), against GVT results, the criteria for the verification of the TM adjustments are frequency deviation and mode shape quality (Figure 3, top left). When evaluating the numerical model against the data from FVT measurements, in-flight frequencies and damping are evaluated versus flight velocity (Figure 3, top right / bottom).

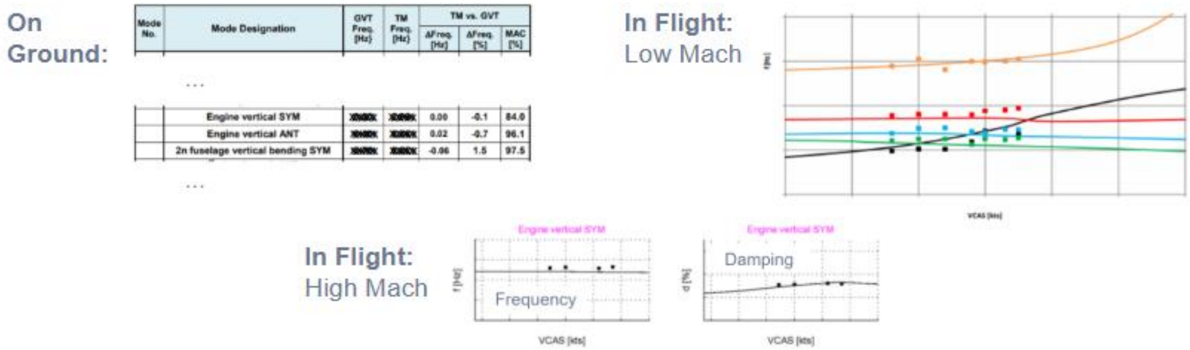

Figure 3. Comparison of test data and simulation data

2.2 Motivation for Process Improvement

While the current process has shown its value and is satisfying the accuracy needs for past aircraft developments, there is great potential for an improvement of the model adaptation process. The current process is based on sequential consideration of test results, i.e. test on ground, calibration flight (low Mach number), flight test at high Mach numbers (cruise up to dive). The adaptations are mainly based on a manual process, and are focussing on relevant modes in the low frequency range, as exemplarily shown by the example of the transfer function Rudder to Cockpit presented in Figure 4

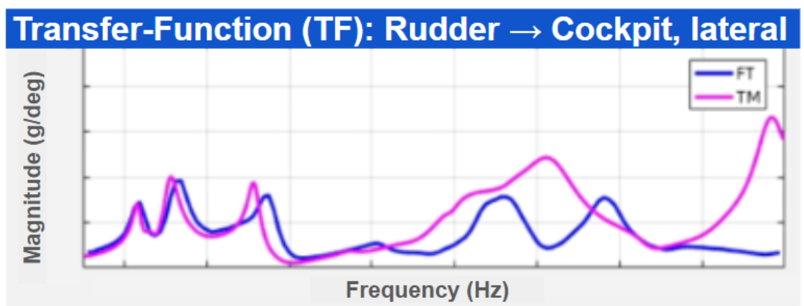

Figure 4. Comparison of transfer function Rudder to Cockpit from FVT and adapted model

A future process needs to be faster in converging on a solution proposal and should be able to consider simultaneously larger frequency range at several aircraft configurations, e.g. fuel vectors. This includes the capability to show good correlation of transfer functions between several measurement points and excitations. Additionally, more detail in choosing the adjustment parameters and the capability of treating a much higher number of parameters at the same time, i.e. more sophisticated than a beam approach, is essential.

All these considerations lead to the conclusion that dynamic model adjustment is considered to be an optimization task, to be performed on a full aircraft model. To this end, a new process for Dynamic Model Adjustment Optimization (DynAOPT) is presented, based on NASTRAN SOL 200, the optimization and design-sensitivity module inside NASTRAN, Figure 5.

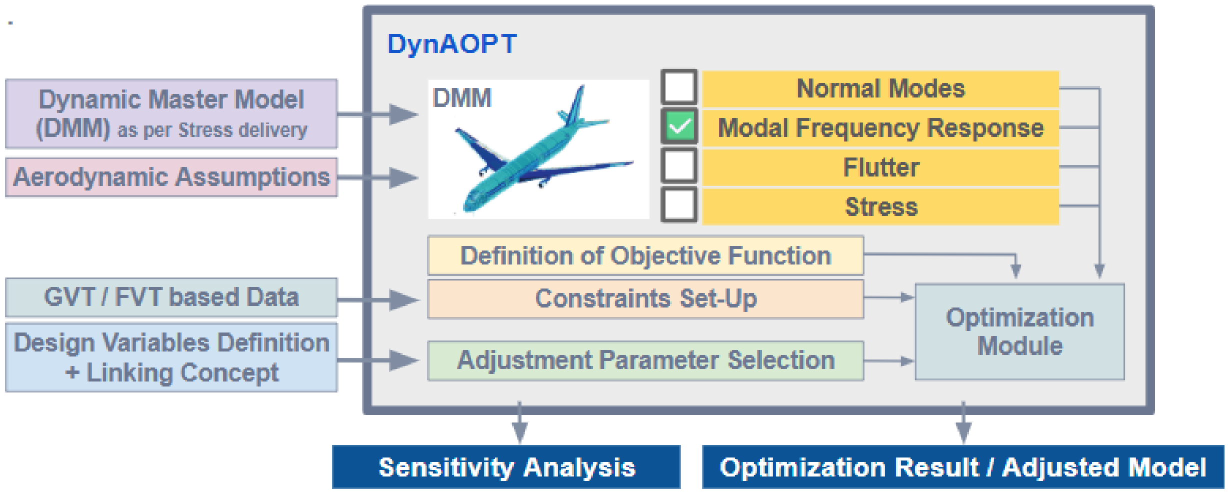

Figure 5. The DynAOPT process

The tool can be used for identifying the sensitive areas to improve a certain mode. The same tool is then capable to run the optimization, potentially with an approach linking the adjusted or modified design variables, thus reflecting the conclusion from the sensitivity analysis.

The main advantage of this process is further that several options are available to find an adequate solution. This means that the adjustment can be done by addressing the transfer function deficiencies via a Modal Frequency Response analysis, by imposing frequency constraints on certain modes via a Normal Modes analysis, by constraints tracking selected modes versus speed in a Flutter analysis, or by a combination these numerical methods just by defining appropriate constraints. Additionally, stress constraints can be included into the optimization to consider loads-related boundary conditions, Figure 6.

A major aspect of the new process is furthermore the ability to extend the optimization-based adaptation process to include data from flight tests.

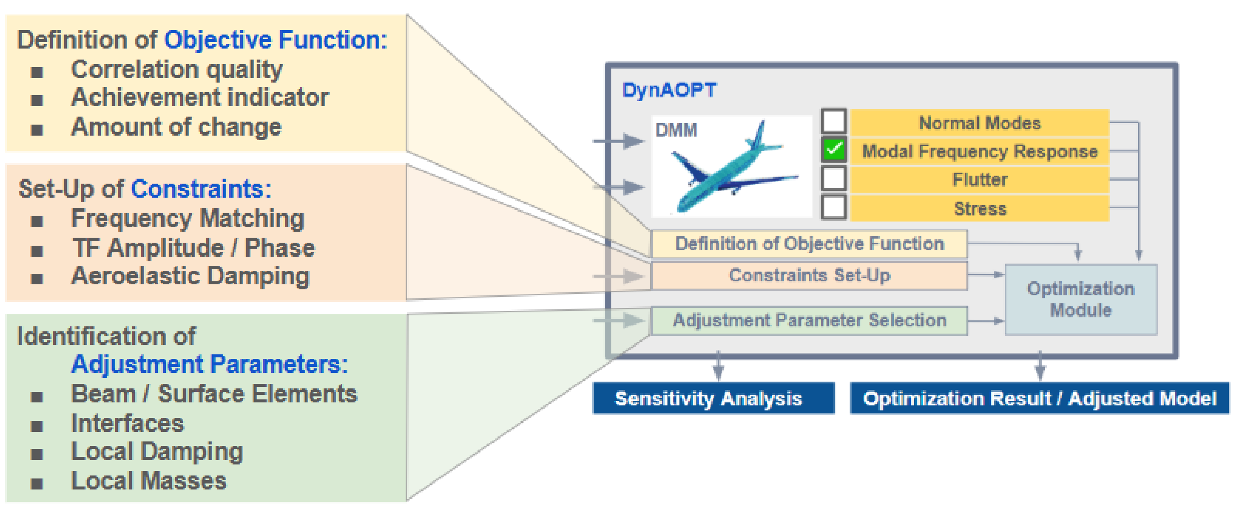

Figure 6. Optimization procedure in DynAOPT

2.3 Application on a Test Aircraft

The following paragraph shows a sample application of the DynAOPT process with data from the GVT of a civil transport test aircraft. The aircraft has been equipped with approximately 180 acceleration channels, as shown in Figure 7.

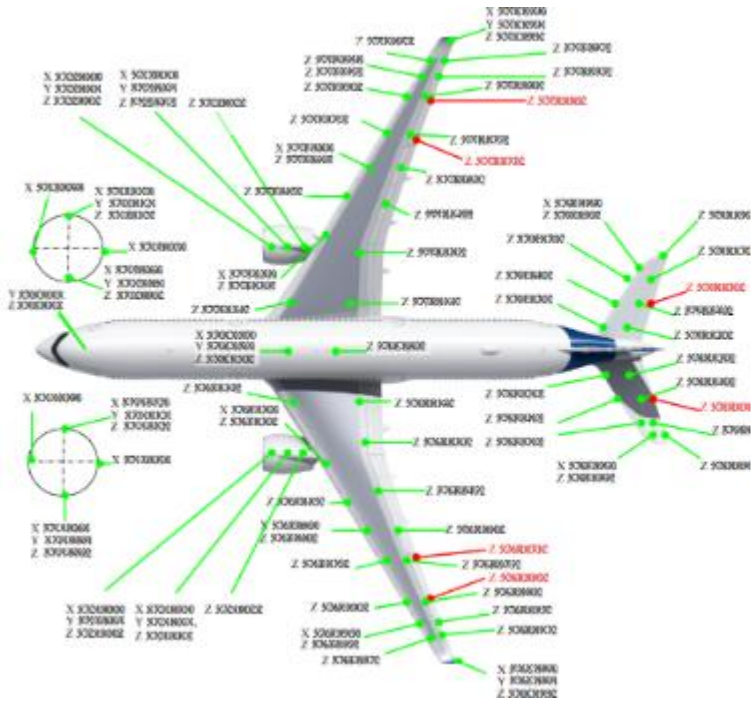

Figure 7. Sensor plan of test aircraft

The transfer function Rudder to Cockpit has been recorded based on a sweep excitation of the rudder, see Figure 8.

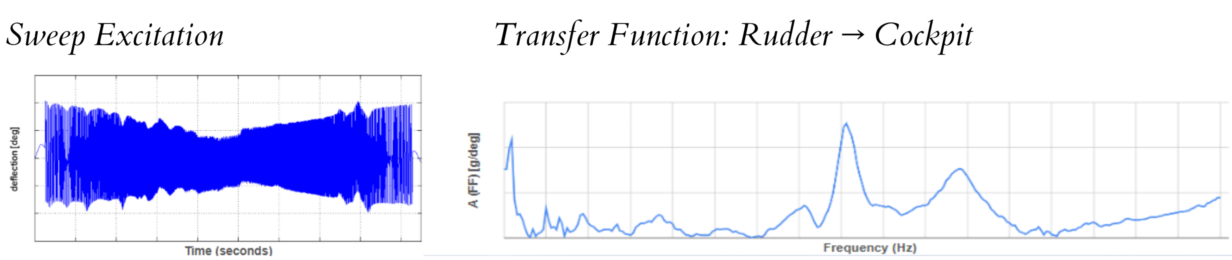

Figure 8. Excitation and recorded transfer function

The target of the investigations was to achieve a good correlation of test data versus the data of the theoretical model, also in the higher frequency range, i.e. from 6 to 8 Hz, while maintaining the quality of the correlation in the low frequency domain.

To achieve this proof of concept, it was decided to focus on the lateral aircraft behaviour, a decision which was driven by the experience that vertical and lateral behaviour can usually be de-coupled. Transfer functions under consideration are first the VTP tip acceleration caused by rudder excitation, measured on ground, and second the cockpit acceleration caused by rudder excitation, measured both on ground and in flight.

Sensitive parameters and proposals for solutions are determined via an optimization. The following options for design variables have been analysed:

- Stiffness (all directions) of VTP and Fuselage, respectively all components
- Structural element damping coefficients of VTP and Fuselage, respectively all components depicted in the diagrams below
- Combination of stiffness and damping
- Additional conjunction elements addressing stiffness and/or damping
- Mass distribution changes

Comparisons have been performed with optimizations without move limits of the design variables (stiffness, damping), and optimizations imposing move limits on the design variables.

Figure 9 shows the results of the optimization of the dynamic model based on the ground data, indicating the imposed constraints for the optimization by the yellow and dark green points in the diagram aiming to meet the test result given by the blue line. The reference / initial simulation result is indicated by the red line. The optimized solution is a best compromise between all imposed constraints. In the frequency range of interest between 6 to 8 Hz, a good match could be achieved for the acceleration level, removing the very high acceleration peak proposed by the DMM which was not observed during test. For the lower VTP bending frequency, the peak frequency matches better between model and measurements, while the match of the amplitude at that frequency becomes worse. It can be seen that a reduction of the move limits for the design variables implies less correlation quality. In Figure 10, Optimization run opt_b03.1_01 is much closer to the targets compared to run opt_b03.2_01.

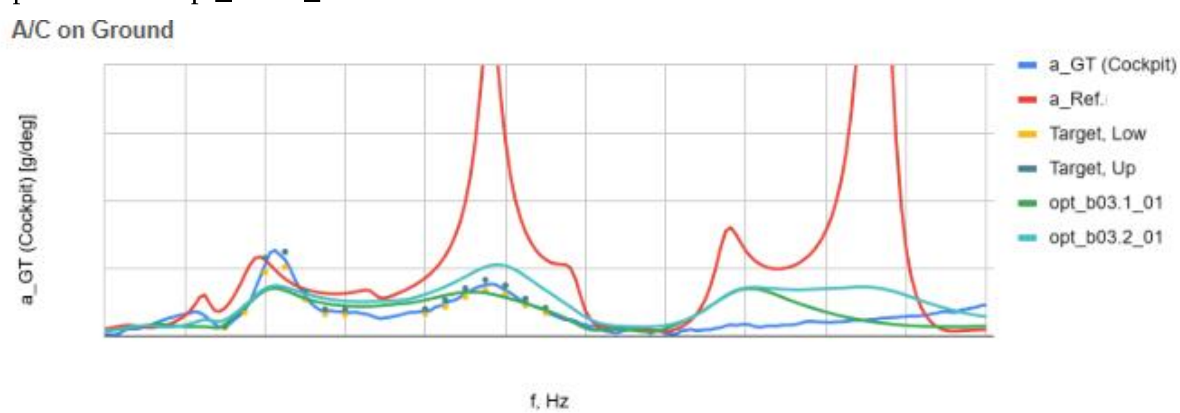

Figure 9. Optimization results based on ground data (blue = unlimited, red = limited, green = unlimited, turquoise = limited)

In addition, a limit on the permitted variation of the design variables can be shown to result in a different distribution of the design variables, see Figure 10.

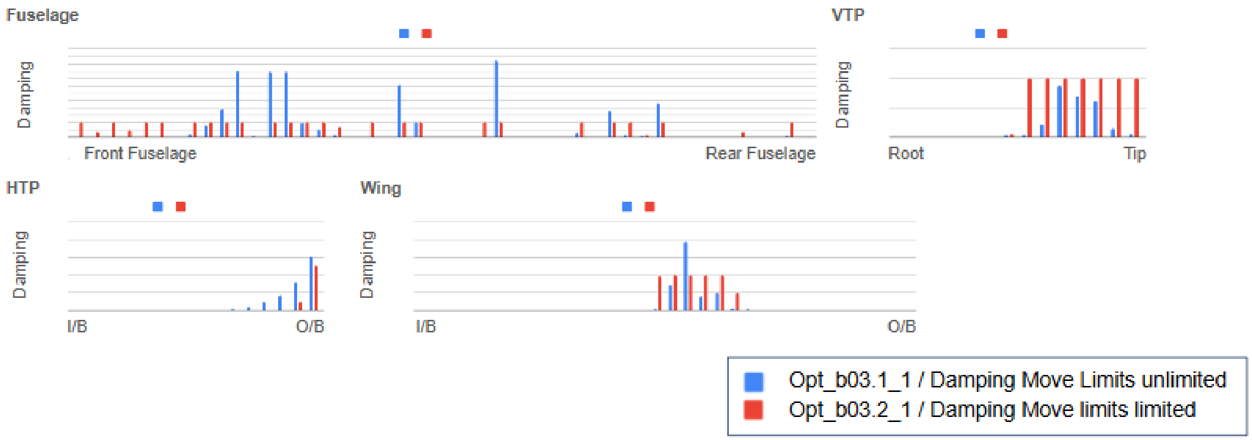

Figure 10. Influence of move limits on the distribution of design variable

In a second step, the model is adapted based on in-flight data. Figure 11 shows the transfer function for rudder input and cockpit acceleration for the optimization runs. The blue curve is depicting the test result whereas the transfer function of the simulation model is shown with the initial (not adjusted) set-up (red curve) in comparison with the adjusted / optimized solution (green curve).

A very good agreement can be seen between flight test data and simulation in the frequency range of interest, with imposed amplitude constraints (depicted as dots in the diagram). It should be noted that the correlation of the amplitude is also much better in frequency range which was not constrained.

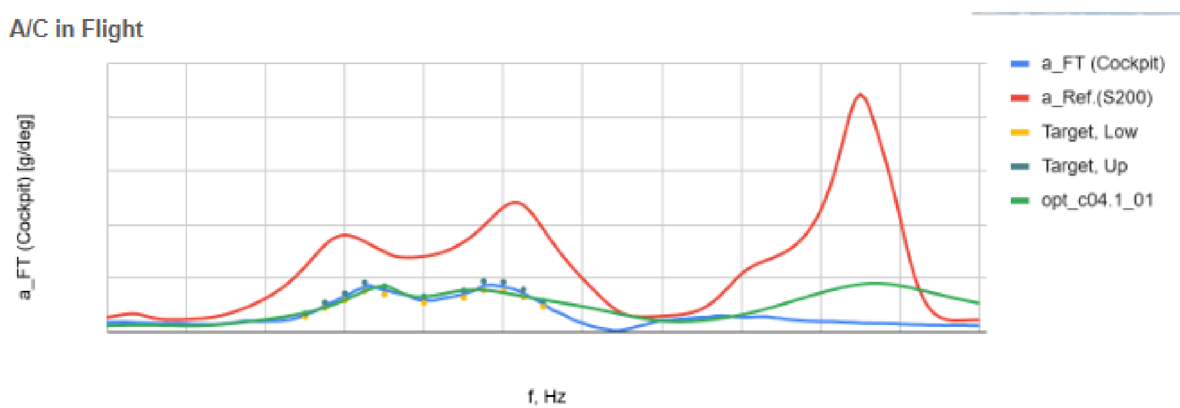

Figure 11. Optimization results based on in-flight data

Looking at the design variables, the following conclusion can be drawn: Optimization runs done on the basis of different test data sets, here ground- respectively flight test, potentially are activating different design variables to achieve a similar correlation result in a certain frequency range. On the wing, different design parameters are used to match either ground- or flight test results, whereas on the VTP partially the same parameters are proposed in the same direction with a similar quantity or even can go in opposite directions.

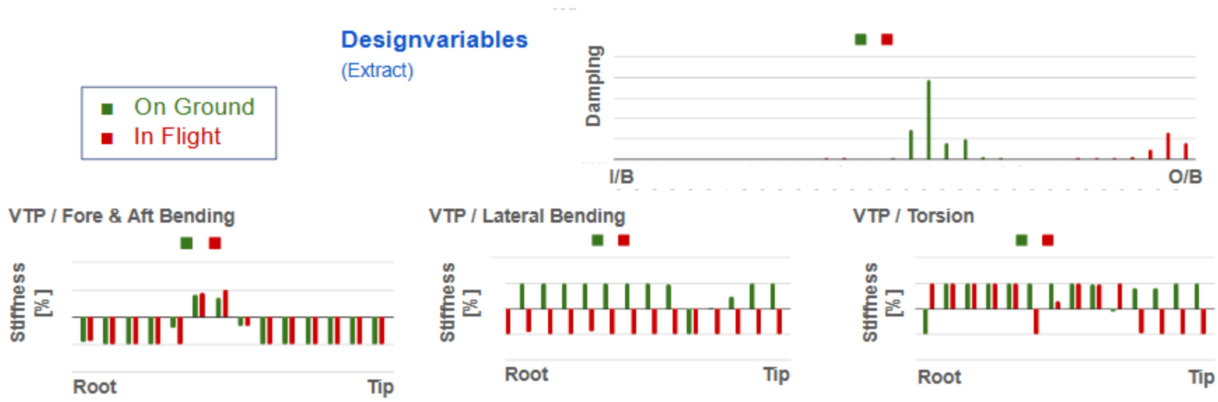

Figure 12. Change of design variables based on ground and on in-flight data

The reason for the fact that separated optimization runs propose different solutions is the complex design space. This clearly points out that a simultaneous approach is needed to satisfy all conditions and to come to a single converged solution.

Summarizing, it can be stated that for the test aircraft, an adjustment environment has been established to improve the simulation model, aiming to match ground and flight test results. The tool ‘DynAOPT’ is used for the dynamic model adjustment in context with optimization. It is based on NASTRAN Sol 200 and is seen as the appropriate solution allowing to combine several numerical approaches (normal modes, modal frequency response, flutter, loads, stress) with a large variety of optimization options without the need of data transfer between different tool environments. Independent of the approach, the case study underlines the fact that identification of the right adjustment parameters is the key for the success of the optimization and the quality of the results.

3 AEROELASTIC OPTIMIZATION

3.1 Aircraft Model

The following section describes the structural optimization of a transport aircraft wing with the goal of increasing the flutter speed of the aircraft. As outlined in Section 1, the approach is to modify components of the structure with minimum mass increase, minimum modification of the given aircraft structure, and satisfying all local strength constraints. For the given example, possible adaptations of the engine pylon structure and of the wing skin have been selected.

The model used is a variant of the DLR D2AE model [1]. The D2AE is a numerical transport aircraft configuration developed for aeroelastic and aeroservoelastic investigations at the DLR. The wingspan is 42.5 m, resulting in an aspect ratio of 12.4. The wingtips can be folded to stay within the airport box of 36 m. The finite element model of the aircraft is a so-called global finite element model (GFEM), which is of comparable detail to the DMM model used in Section 2. The mass model and the stiffness model of the structure, as well as the aerodynamic DLM grid and the splining between the structural and the aerodynamic model, are generated separately in the DLR model generation process cpacs-MONA [2] and combined to form the full aircraft FE model. Structural sizing is done inside NASTRAN as a structural optimization based on a load analysis including approximately 25 selected load cases.

Figure 13. CPACS model (top), GFEM stiffness model (bottom left), GFEM mass model (bottom right) of D2AE

The D2AE model is pictured in Figure 13, on the top the CPACS model showing the geometrical layout of the aircraft, on the bottom the stiffness model (left) and the mass model (right) of the finite element model of wings, fuselage and empennage.

The fuselage of the aircraft model is built up of beam elements, the blue shell elements are for visualization only and have no physical properties assigned. The wing box is modelled with shell elements (red) representing the skin and spars of the wing. The wing box is further reinforced by stringers that are modelled with beam elements. No structure of the movables such as ailerons or flaps are represented in the FE model, the leading and trailing edges are only included for illustrative purposes and for coupling to the DLM model; the engines are modelled as point masses on a pylon, the fairings are included for visualization only. The GFEM model is optimized for selected static load cases, so a pre-sized model can be obtained for different mass configurations.

For the spars and skin of the wing anisotropic materials are defined to support composite material modelling. A NASTRAN MAT2 card is used to define these linear properties of the shell elements. For the beam elements, standard MAT1 cards are defined. It is important to note that due to the separation of the mass and stiffness model, the materials have a density of zero. In the optimization process described below only the thickness defined by the MAT2 cards will be varied, keeping the given material properties constant.

The used mass configuration is the operating empty mass with zero fuel (MOOee) configuration. Due to the density of zero defined for the elements, the masses are not a result of the thickness of the elements but rather added as concentrated mass points on the FE grid points. On the wing, additional trim masses with a total mass of 394 kg have been added manually to create an artificial flutter instability, since the standard D2AE configuration is not designed to be unstable by itself. The masses on the trailing edge are 21 kg each and the outermost pair on the trailing and leading edge are 25 kg. This mass distribution leads to a flutter point which is deliberately chosen between the dive speed v_D of the aircraft and 1.15 v_D.

For the aerodynamic modelling, the NASTRAN DLM is used, defined for the lifting surfaces by NASTRAN CAERO1 cards. The movables are modelled in the aerodynamic grid, but are not used in the aeroelastic optimization task.

After all parameters were defined, the study was performed with the 2023.4 version of MSC NASTRAN. For the flutter investigations of the full aircraft, the number of vibration modes was determined by a convergence study. It was found that 25 modes, respectively modes up to a frequency of 20 Hz, are required to obtain consistent results. The resulting frequency and damping plots for the full aircraft flutter analysis of a generic case (Ma = 0.7, sea level) are pictured in Figure 14. Two modes become unstable at velocities of 351.1 m/s and 352.5 m/s. Both flutter cases are driven by modes mainly involving motion of the wing tip. The aim of generating a flutter mode to be optimized could thus be achieved.

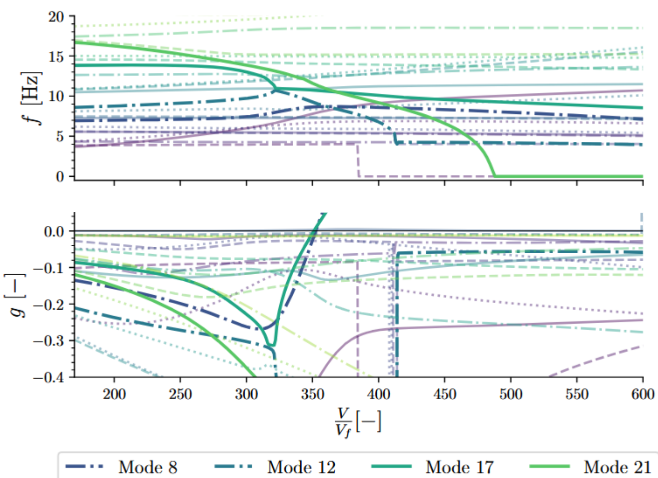

Figure 14. Frequency and damping plot of the D2AE with 25 vibrational modes

However, what stands out in the flutter plot are the discontinuities in the solution slightly above the flutter speed V_f. The actual reason for these discontinuities is unknown, but it can be assumed that the cause is similar to the one described by van Zyl in [3] who identified this behaviour as a result of the specific implementation of the p-k method.

After a review of the results and a discussion of the flutter behaviour, it remained unclear if and in which way the discontinuities in the solution as well as the uncertain behaviour of the mode tracking would impede the iterations of the optimization. The decision was thus made to simplify the optimization model to that of a fixed wing. This is justified, because as the flutter modes do not include much full aircraft motion, the flutter mechanism is retained on the fixed wing.

3.2 Wing Model

To simplify the model, the wing was isolated and a half model was used. The wing was fully clamped at the wing box to eliminate the influence of fuselage and empennage masses. The resulting model is pictured in Figure 15, left. Further, the slender body aero elements that had been used for the fuselage were removed so new CAERO1 fields had to be defined for the missing area. Since the movables are not used in the process they were also removed from the aero grid. While it had not been a problem for the full aircraft, the pylon panels were removed because they interfered with the wing panels which can lead to badly conditioned matrices within the DLM. The aero model is shown in Figure 15, right.

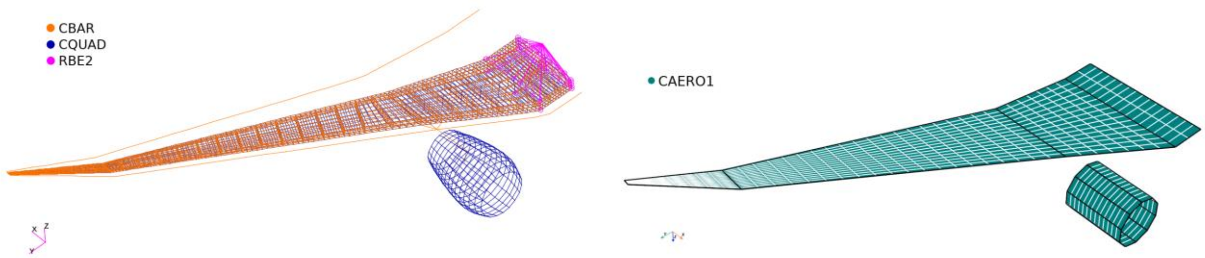

Figure 15. Structural model (left) and aerodynamic model (right) of isolated wing

The flutter curves of the reduced model were compared to those of the full aircraft, see Figure 14 and Figure 16. For the wing, there is only one flutter mode that becomes unstable. Presumably symmetric and antimetric flutters modes evolved for the full aircraft driven by the same local mechanism represented by the single wing. The flutter velocity is almost identical to that of the full aircraft, which under these rather rough simplifications is a good result. Further, a similar behaviour of aircraft and single wing can be observed in the damping curves. Even though not as strongly developed, the damping of the unstable mode 6 (isolated wing) in Figure 16 first becomes more stable before the coupling drives it to the unstable region, similar to the behaviour of mode 17 (full aircraft) in Figure 14.

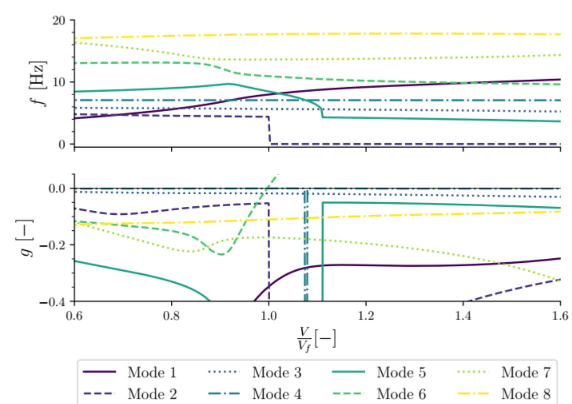

Figure 16. Flutter curves of the reduced model

The flutter frequencies of the isolated wing are slightly lower than those of the full aircraft. By fixing the entire wing box and removing the masses of the rest of the aircraft, stiffness was added and mass was reduced respectively, so it is plausible that wing frequencies increase.

The downside that came with the model reduction was the discontinuity migrating exactly into the range of the flutter velocity, see Figure 16, left. Thus, parameter studies were conducted to gain insights into the sensitivity of the flutter solution with respect to simulation parameters. In these investigations, different flutter solvers available in MSC NASTRAN (k, pk, pks) were applied. Steps of reduced frequencies k were varied, as well as the available interpolation methods for the generalized air forces (GAFs, linear spline, cubic spline). A finer resolution of the reduced frequency did not change results but increased computation times. The velocity resolution affects the mode tracking but has no major influence on the solution. The chosen Mach number, however, exhibited a strong impact on the discontinuity. The most robust solution in the optimization loop was obtained using the so-called pks method, a non-iterative variant of the pk-method.

Using the isolated wing model, the modal basis could be reduced to 12 modes, maintaining the flutter mechanism also seen on the full aircraft. With this set up, the optimization will now be conducted.

3.3 Optimization Set-up

For the study of the design fields, the input has been available from the original sizing of the wing structure in the cpacs-MONA process. The design variable set of this process has been adapted for the algorithm study by removing the ribs as design variables as well as those inner part of the wing which would be inside the fuselage. A picture of the design fields is presented in Figure 17, left. The black elements represent the excluded elements. The design fields are defined between each rib and are divided mid-chord. The front and rear spar are included, divided by the ribs as well. The design variable is the skin thickness of the elements.

The second set of design variables includes the pylon structure, pictured in yellow in the wireframe picture, Figure 17, right. The pylon is modelled as a beam, discretized in 10 sections, and two V-shaped attachments to the wing structure, also modelled as beams. For this set, the thickness of the material could not be applied as a design variable, so the Young’s Modulus has been directly used instead.

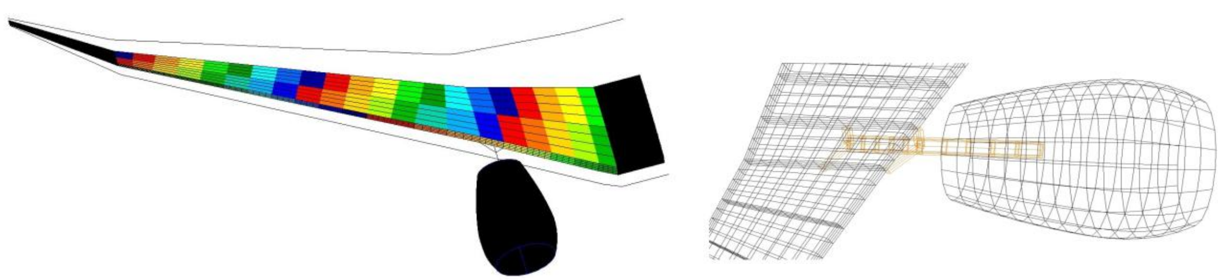

Figure 17. Design fields of the D2AE wing model and on the pylon model

To study the applicability of the available optimization methods, the IPOPT algorithm and different methods from the MSCADS library have been tested on the wing model. In this process, the optimization parameters have mostly been left as the default values. Aside from the used algorithm itself, important parameters are the move limits and the objective function with its criteria of convergence. At this point the aforementioned separation of the mass and structural model become an issue. An additional density can be assigned to the design elements to introduce mass changes, but those changes proved not to be significant enough to be a reliable incentive for the optimizer. By looking for a better conditioned objective function, the mass was abandoned and instead the volume of all elements was minimized. This provides the advantage of directly calculating the objective function based on the FE-changes without need for additional modifications, in contrast to the mass function approach. The volume function further offers the advantage of evaluating the summarized structural changes compared to the initial design and thus calculating meaningful relative changes. The downside of using the volume is the missing influence of the density. Therefore, once materials of varying density are utilized, the objective function will become flawed.

The optimization goal was to increase the flutter speed with a minimum mass increase. These two objectives are, as a rule, contradictory. A possible approach could be to define a multi-objective cost function and to apply weighing functions to achieve an optimum compromise. However, as the direct optimization of the flutter speed showed convergence difficulties for the current model, a different approach was followed, using damping as a constraint.

However, in the definition of response and constraints, it was found that the flutter velocity is not a very functional constraint. The initial idea to constrain the damping with a function of the velocity, as suggested by Ringertz [4] and Stanford [5], could not be implemented because it was not possible to access arbitrary pairs of velocities and the respective damping. The optimization task was thus formulated in a different way: In a preceding parameter study, a 5% increase of the flutter speed was found to be achievable with reasonable structural modifications. The optimization was now expressed as follows – for a velocity up to 5% above the flutter speed of the original model, minimize mass under the constraint that the damping for all modes remains positive, at given velocity points.

The flutter response requires the flight condition inputs that must be identical to those of a detailed flutter analysis input. Then a subset can be defined for the velocities at which the damping values are provided for the constraints. With a flutter velocity of 355 m/s the subset was defined from 350 m/s up to a velocity of 373 m/s to be able to achieve an increase of 5%. Additionally, a coarse resolution was used down to 200 m s to prevent hump modes. The results were again normalized with the VREF parameter.

To properly visualize the results some post processing is required. NASTRAN offers options to control the output of the optimization run. The level of information the user can access ranges from no output at all over objective and constraint values down to gradients and one-dimensional search information. To gain an insight of how the optimizer proceeded, a python script was written to visualize the flutter plots of each iteration. The plots made it possible to quickly check if modes were tracked incorrectly. Further, it can be seen how the optimizer is reaching the goal and how the flutter behaviour itself might change

The constraint offset and the associated move limits were set according to the results of the parameter study. The optimizer could be directed to provide a controlled approach. After evaluating the results of the method study, the SQP algorithm of the mass objective function was used in an attempt to bring more clarity to the convergence decision logic. It also was found to be the fastest algorithm of the five available algorithms. The so-called move limits for the design variable, limiting the relative change of the design variable within one design cycle turned out to be quite important. An issue that was introduced with the move limits was the forced soft convergence. Occasionally, the changes in the design variable were so small due to the move limits that the so-called soft convergence was satisfied. This alone is not a problem, but in combination with the small weight changes, the hard convergence was triggered. However, the design was still far from feasible, so the convergence criteria were lowered by a power of 10 to 0.0001 of relative design variable change. To enforce a convergence to a feasible solution, the minimum design variable change was set to 0.001, so one magnitude higher than the convergence limit.

For reasons of convergence, a constraint should not be zero in the optimization problem, see the NASTRAN guide for background and methodology of the normalization of constraints in the optimization. Thus, as the damping at the flutter point is zero by definition, damping values are offset by a predefined factor and then scaled. This was done using a NASTRAN internal variable.

Optimizations runs were performed for the objective function of minimum mass, and for the alternative formulation of minimum volume (see above). Table 2 lists the final results of the mass objective function and Table 3 the ones of the volume objective function. As expected, the change of mass is very low compared to the initial weight of 13100.45 kg. Still, setting the results in relation to each other, the MMFD generated the heaviest design with three times the mass increase as the other algorithms. However, the MMFD algorithm required only half of the iterations with only 11 detailed analyses in contrast to the second least 23 of the SQP. It is worth mentioning that the difference between the SLP and SQP is only 2 iteration cycles, even though the SQP is supposed to outperform the SLP due to the reduced number of iterations. The results of the SQP are nonetheless better compared to the SLP.

algorithm	MMFD	SLP	SQP	SUMT	IPOPT
Δm [t]	0.35	0.10	0.10	0.12	0.10
n_{iter} [-]	11	25	23	27	25
x_{max} [-]	0.437	0.049	-0.011	0.014	0.002
g at 1.05 V_f [-]	0.0131	0.0014	-0.0007	0.0004	0.00006

Table 2: Results of optimization algorithms with mass objective function

Continuing with the results of the volume objective function in Table 3, the MMFD is no longer a clear outlier. The MMFD achieved the second lowest value with a volume increase of 0.51% shortly after the SLP with 0.50%. It is surprising that the SLP outperformed the SQP, this time with actually fewer design cycles and a better objective value. The constraint was however better satisfied by the SQP. While the SUMT did not reach the threshold with the mass objective function, it now achieved a slightly negative damping. As will become visible later, the identical results of the IPOPT are no coincidence but truly identical. It is not known why the change in objective function did not lead to any changes in the results.

algorithm	MMFD	SLP	SQP	SUMT	IPOPT
ΔVol [%]	0.51	0.50	0.64	0.58	0.54
n_{iter} [-]	25	25	27	25	25
x_{max} [-]	0.052	0.048	-0.0012	-0.007	0.002
g at 1.05 V_f [-]	0.0131	0.0014	-0.0007	-0.0002	0.00006

Table 3: Results of optimization algorithms with volume objective function

In general, all algorithms achieved the aim of increasing the flutter velocity by 5 % with acceptable tolerance for both variants of objective function. Figure 18 shows a result for the development of the optimization history for the example of the SQP optimization algorithm with the volume objective function. While there is a lot of detailed difference between the results for the various algorithms and objective functions, the global behaviour when represented as a flutter curve is very similar for all approaches.

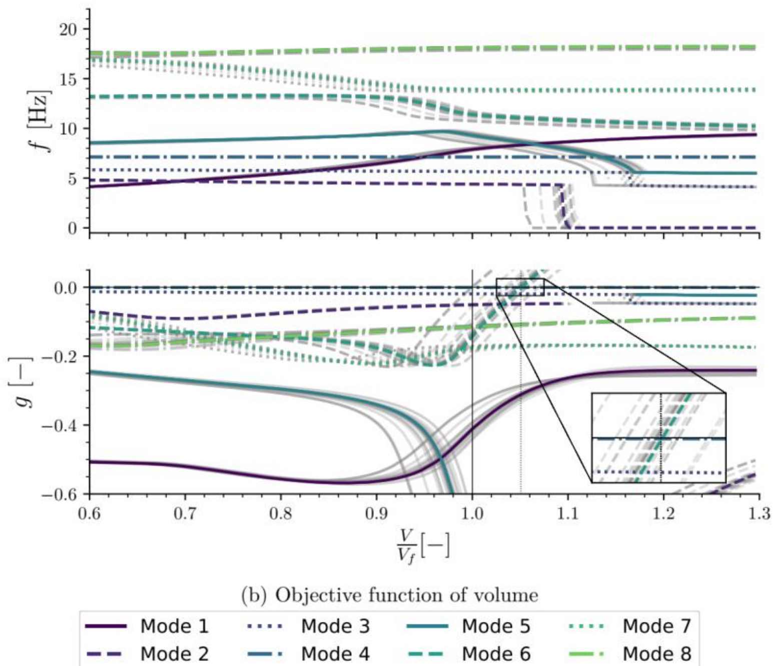

Figure 18. MSCADS SQP flutter curve history

In the following, the relative changes of the thickness are visualized in Figure 19. The fact that the MMFD did not handle the mass response very well is also clearly visible in the structure. It is very distinct from the other methods, as the entire wing box is thickened by at least 4 %. Aside from that, all algorithms increased the skin thickness at 3/4 of the wing span by approximately 12 %. When looking back at the mode shape of the flutter modes, this is very reasonable, as this position exhibited the largest bending deformation.

When comparing results for mass and volume objective functions, the MMFD and the IPOPT produced comparable results for both functions. The SQP shows the biggest differences. The right-hand (i.e. volume function-driven) design of the SQP indicates a much more nuanced center section of the wing with a reduced red area of maximum increase. The same picture can be found on the upper side with a generally smaller area of increased thickness.

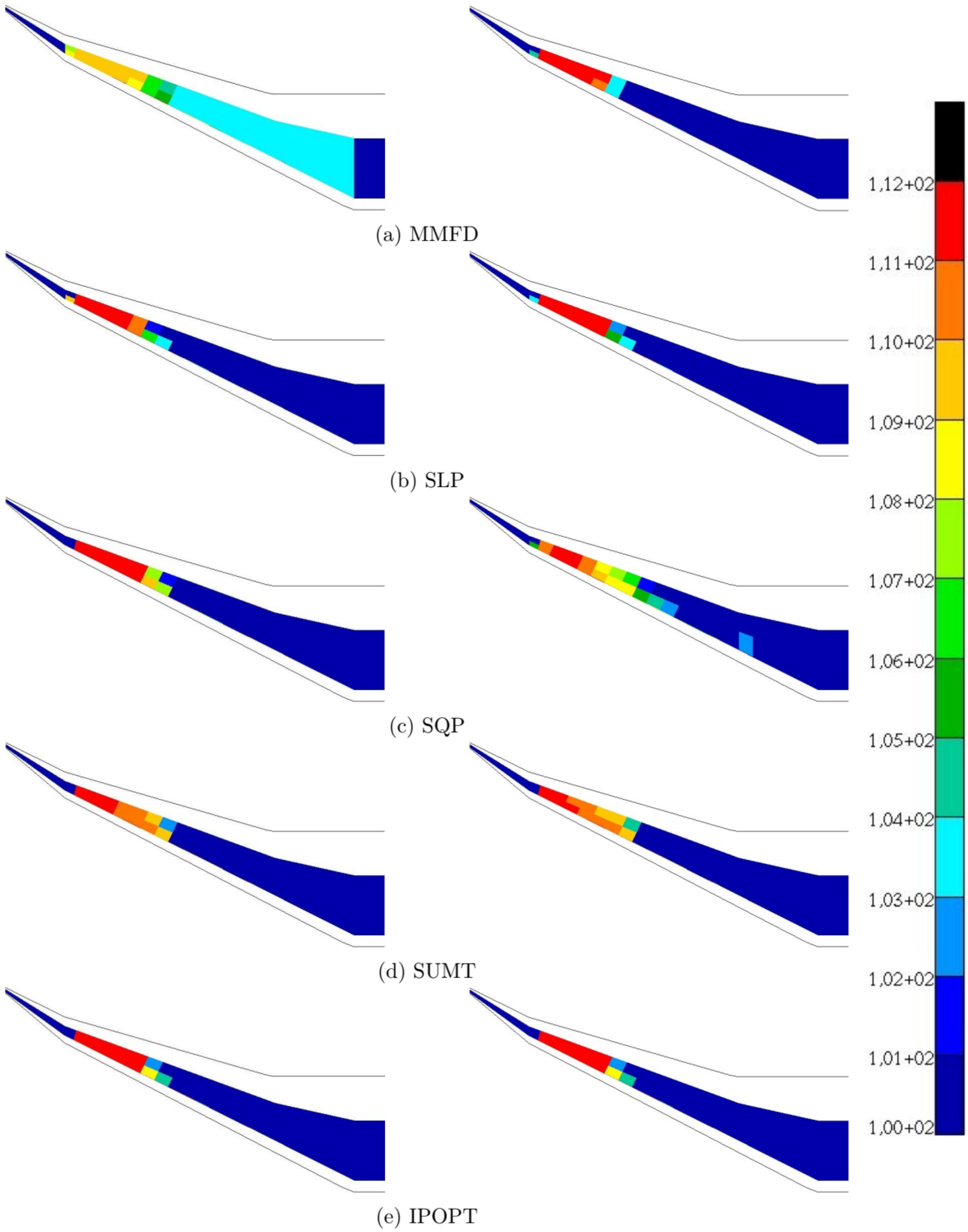

Figure 19. Relative changes of upper skin thickness with objective function of mass (left) and volume (right)

To summarize, both objective functions produced adequate results. The volume objective function proved to be more robust with regard to the optimization algorithms. However, considering that the mass is not a very suitable response to choose in combination with this model setup, the results are still remarkably close to the volume driven designs. The structural changes show a clear trend of stiffening the area of largest bending deformation of the flutter mode, which is reasonable. In terms of the algorithm, there is no most optimal design. All designs lead to a volume increase of 0.5% to 0.65%. Since the wing is empty, it is valid to assume that the volume change is comparable to the mass change. So applying the volume changes to the wing mass of 13100.45 kg the weight increase is 65 kg to 84.5 kg for a 5% increase of flutter velocity.

In addition to the structural optimizations performed on the wing design fields, the optimization was also executed using the stiffness of the engine pylon. However, it was found that the specific flutter mechanism of the wing which is subject to this study is not sensitive to pylon stiffness.

3.4 Flutter Check with Full Aircraft

The final question to answer is whether the changes of the wing model produce comparable results when applied to the aircraft model. The results of the MMFD with the volume objective function were considered a good compromise of all algorithms results. Hence, the changes of the optimized right wing were mirrored onto the left wing and implemented for the aircraft model input deck. A flutter analysis was then performed comparing the reference aircraft and the aircraft with the optimized wing. The results can be seen in Figure 20. The flutter velocity of the full aircraft was increased by 4.62%. This does not quite reach the 5 % that were set for the isolated wing model but is still an improvement of similar magnitude. Further, both flutter modes of the full aircraft were affected by the changes. Other modes than the flutter modes were not visibly affected. Summarizing, the acting flutter mechanism allowed a very efficient transfer of the optimization results from the isolated wing to the full aircraft.

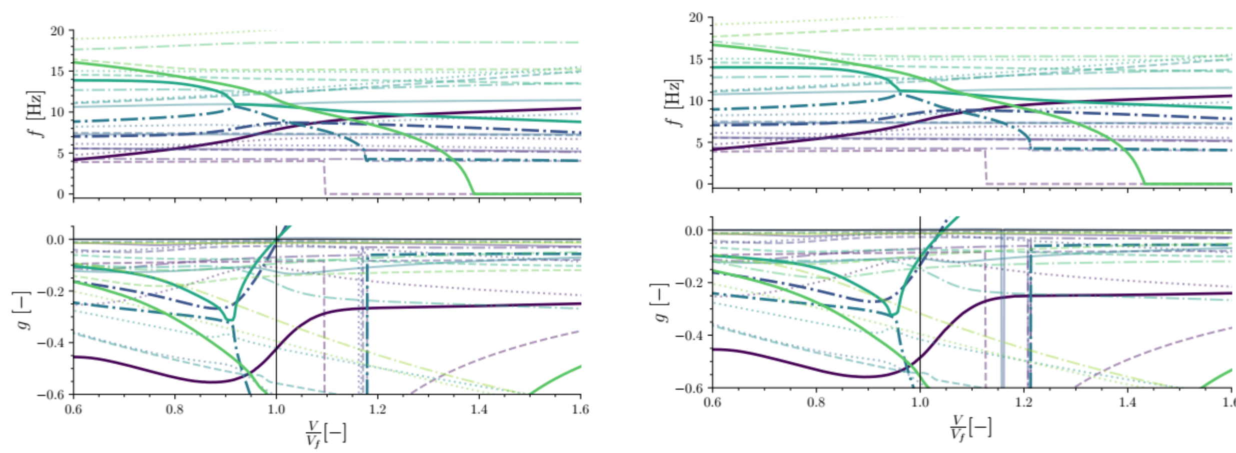

Figure 20. Frequency and damping plots of reference aircraft (left) and optimized configuration (right)

4 CONCLUSIONS AND OUTLOOK

Optimization of aeroelastic models is an important tool along the lines of an aircraft development, both for the adaptation of numerical models to match test results from ground tests and flight tests, and to suggest design changes to remove limits set by aeroelastic constraints, such as flutter margin enhancement.

In the frame of next generation development, an adjustment environment has been established to improve the simulation model aiming to match Ground- & Flight Test results. For dynamic model adjustment in context with optimization, this powerful tool ‘DynAOpt’ is based on NASTRAN Sol 200 and is seen as the appropriate solution allowing to combine several numerical approaches (normal modes, modal frequency response, flutter, loads, stress) with a large variety of optimization options without need of data transfer between different tool environments. The approach has been successfully applied during project development work, mainly by demonstration of transfer function correlation. The work shows that the identification of the right adjustment parameters is the key for the success of the optimization and quality of the results.

Further improvements of the optimization process, aiming to achieve the highest quality of the adjusted dynamic model, are proposed via the combination of different aircraft configurations, i.e. different fuel vector cases, ground- and flight boundary conditions, gaining experience with constraint setting and a refined definition of the objective function.

The NASTRAN-based optimization was also shown to be successful for the increase of the flutter speed by modification of the wing structure, with a minimum of mass increase. For reasons of complexity, the optimization study was restricted to an isolated wing. For that wing, all optimization algorithms available showed the same global trend of thickness changes over the wing with only a few outliers. The aim of a 5 % increase of flutter velocity was mostly achieved with the wing design model. The pylon design model was analyzed separately but did not succeed in increasing the flutter velocity. After reviewing all parameter studies and design models, structural changes of the wing design model were applied to the aircraft model. The modifications achieved a 4.62 % increase of flutter velocity with approximately 130 kg of additional mass. The goal of increasing the flutter velocity with minimum increase of mass was therefore achieved.

However, the limitation of staying within the NASTRAN environment led to several shortcomings. First, the mass as an objective function could not be effectively used due to separated mass and stiffness models. The resulting mass changes are only a result of the volumetric changes that are specifically for this empty mass configuration applicable to the mass changes. Furthermore, the goal was not achieved by directly optimizing the entire airplane structure. Instead, the workaround for the error-prone flutter analysis was to reduce the model, which included significant manual work and modification of the input decks

A future goal is to include the flutter optimization as a design tool directly into a multidisciplinary optimization (MDO) loop. This requires a lot of development as currently a lot of manual effort is involved to gain an understanding of the relevant flutter mechanism.

REFERENCES

[1] Klimmek, T., Schulze, M., Wöhler, S. (2022): Development of a Short Medium Range Aircraft Configuration for Aeroelastic Investigations using cpacs-MONA. Deutscher Luft- und Raumfahrtkongress 2022, 27.-29.09.2022, Dresden. https://elib.dlr.de/194675/

[2] Klimmek, T., Schulze, M., Abu-Zurayk, M., Ilic, C., Merle, A. (2019): cpacs-MONA – An independent and in high fidelity based MDO tasks integrated process for the structural and aeroelastic design for aircraft configurations. International Forum on Aeroelasticity and Structural Dynamics, IFASD 2019, Savannah, GA, USA.

[3] Van Zyl, L. H., and Maserumule, M. S., “Divergence and the p-k Flutter Equation”. Journal of Aircraft, Vol. 38, No. 3, 2001, pp. 584–586. https://doi.org/10.2514/2.2805

[4] Ringertz, U. T., “On structural optimization with aeroelasticity constraints,” Structural Optimization, Vol. 8, No. 1, 1994, pp. 16–23. https://doi.org/10.1007/BF01742928, URL http://link.springer.com/10.1007/BF01742928.

[5] Stanford, B. K., “Role of Unsteady Aerodynamics During Aeroelastic Optimization,” AIAA Journal, Vol. 53, No. 12, 2015, pp. 3826–3831. https://doi.org/10.2514/1. J054314, URL https://arc.aiaa.org/doi/10.2514/1.J054314.

[6] Albano, E., and Rodden, W. P., “A doublet-lattice method for calculating lift distributions on oscillating surfaces in subsonic flows.” AIAA Journal, Vol. 7, No. 2, 1969, pp. 279–285. https://doi.org/10.2514/3.5086, URL https://arc.aiaa.org/doi/10.2514/3.5086.

[7] Hexagon, “Aeroelastic Analysis Users Guide - MSC Nastran 2023.1,” Nastran Userguides, 2023.

COPYRIGHT STATEMENT